Plastic Anisotropy in Aluminium - Effect of Texture and Microstructure

D. JUUL JENSEN and N. HANSEN - Materials Department Risø National Laboratory - DK-4000 Roskilde, Denmark

Abstract

The effects of crystallographic texture and deformation microstructure on the flow stress anisotropy in aluminium are reviewed. The texture is measured by neutron diffraction and the textural contribution to the anisotropy is determined by model calculations. It was found that texture can have very large effects on the anisotropy. However, for most experimental conditions, texture effects alone cannot explain the observed anisotropy. In those cases the non texture part of the anisotropy is caused by microstructural effects, and the relation between development of macroscopically oriented microbands and the "microstructural anisotropy" is discussed. Finally the effects of various materials and processing parameters on the flow stress anisotropy, the texture, the microstructure and on the relative importance of texture/microstructure effects on the anisotropy is discussed.

Riassunto

Si passano in rassegna gli effetti della tessitura cristallografica e della microstruttura di deformazione sull'anisotropia delle tensioni di flusso nell'alluminio. Si misura la tessitura mediante diffusione di neutroni e si determina con calcoli di modello il contributo della tessitura all'anisotropia. Si è riscontrato che la tessitura può avere rilevanti effetti sull'anisotropia. Tuttavia, per la maggioranza delle condizioni sperimentali, i soli effetti della tessitura non spiegano l'anisotropia osservata. In quei casi la parte di anisotropia non dovuta alla tessitura deriva da effetti microstrutturali, e la relazione tra lo sviluppo di microbande orientate macroscopicamente e "l'anisotropia microstrutturale" viene discussa. Infine, si esaminano gli effetti esercitati dai vari materiali e parametri di trattamento sull'anisotropia delle tensioni di flusso, sulla tessitura, sulla microstruttura, nonché la relativa importanza degli effetti di tessitura/microstruttura sull'anisotropia.

Introduction

Optimization of metal forming operations is important to ensure high quality products at acceptable costs. An optimization rely on studies of the metals behaviour during the various processing steps which can form an experimental basis for the development of physically based models combining both process and materials parameters. A thorough materials characterization involves the microstructure, the crystallographic texture and the mechanical properties. In the present paper we shall demonstrate the importance of such a characterization in an analysis of aluminium which has been cold-rolled to different reductions in thickness. For this analysis, the flow stress has been chosen as this property is of technological importance. Anisotropy has been chosen because the causes of anisotropy have not been fully explored. In the analysis of anisotropy it will also be demonstrated how a phenomenological understanding is linked to the development of advanced techniques for microstructural and textural characterization.

Flow stress anisotropy

The flow stress of cold-rolled materials can be highly anisotropic. This has particularly been observed for materials rolled at high strains (e.g. $\varepsilon > 2$) and the effect has in general been ascribed to the effect of the crystallographic texture developing during deformation [1-4]. Flow stress anisotropy may also be found in materials deformed at low strains (e.g. $\varepsilon < 0.5$) which may be related to microstructural effects, e.g. latent hardening [5-6]. Recent results have, however, shown that both at low and high strain, other factors than texture and latent hardening can cause anisotropy [7-8]. The heterogeneity of the deformation microstructures appears to be such a factor. Both the texture and microstructure evolution with increasing strain must therefore be studied in order to understand the occurrence of flow stress anisotropy. This evolution has in the present work been investigated for high purity aluminium (99.996%) and commercial purity aluminium (99.5%). Of special interest has been the effect of initial grain size, which in general is an important parameter in metals forming.

Results

Flow Stress. A series of aluminium materials were cold rolled to various strains in the range 0.05-3.00. From the cold rolled plates, specimens for tensile tests were cut out at fixed angles α to the rolling direction. These angles were: $\alpha = 0, 15, 30, ..., 90°$. For each of these specimens the flow stress was determined at 0.2% offset ($\sigma_{0.2}$).

The results of two of the flow stress measurements are shown in Fig. 1. In the figure the flow stress $\sigma_{0.2}$ is plotted versus the testing angle α. The lower curve is for a cold rolling strain of 0.2 and the top one is for $\varepsilon = 2.0$. At the low strain the flow stress increases with increasing angle α to the rolling direction; in total the material is about 20% stronger at $\alpha = 90°$ (along the transverse direction) than at $\alpha = 0°$ (along the rolling direction). At the high strain, another shape of the $\sigma_{0.2}$ versus α curve is observed. Here the material is weakest at $\alpha = 30°$ and strongest at $\alpha = 90°$; the strengthening corresponds to about 8%.

Texture. The crystallographic textures were measured by neutron diffraction. Compared to the more well known X-ray texture technique, it is advantageous to use neutron diffraction for the present type of investigation, as the neutrons sample complete bulk textures and not only surface textures as the X-rays. This means that the measured neutron textures directly can be compared to the (bulk) flow stress measurements.

The measured texture developments with strain followed the typical pattern for aluminium: at low strains the texture consists of weak rolling components and remaining initial texture components. (If the initial texture in the unstrained condition is almost random, only the weak rolling components are observed). At higher strains the typical high stacking fault energy fcc rolling texture is observed. This texture is rather complex and cannot be described by few discrete orientations. It consists of a continuous series of orientations ranging from $\{110\}<112>$ to $\{112\}<111>$. The notation $\{hkl\}<uvw>$ is used to describe crystal orientations which have the crystallographic $\{hkl\}$ plane parallel to the rolling plane and the crystallographic $<uvw>$ direction parallel to the rolling direction.

For single crystals it is well known that the crystal in general has different properties in different directions and for known orientation of the crystal it is straight forward to calculate the flow stress. For textured polycrystalline materials it is more complex, and the calculations have to rely on theoretical models: The tensile flow stress is expressed as

$$\sigma_{0.2} = M \cdot \tau$$

where τ is the shear stress and M is a relative strength which takes the texture into account. M can be determined using various deformation models. The most commonly used model is the Taylor model [9]. When a polycrystalline metal is deformed, each grain changes shape in such a way as to maintain contact with neighboring grains. To account for continuity of displacements at grain boundaries, it is in the Taylor model assumed that every grain undergoes the same strain as the aggregate in which it is imbedded. To produce these strains, five or more of the twelve slip systems must be operative. The active slip systems are selected to give minimum deformation work. These principles were used to calculate M in the present study. A result is shown in Fig. 2. Here M is plotted versus the angle α to the rolling direction for deformation to a low and a high strain. At the low strain M does not vary very much as a function of α (only about 3%), whereas, at the high strain a large variation is seen (($M_{max}-M_{min}) \sim 10\%$).

The texture contribution to the flow stress anisotropy can be removed simply by dividing $\sigma_{0.2}$ with the corresponding M. Such $\sigma_{0.2}/M$ curves are shown in Fig. 3. If the flow stress anisotropy solely relates to texture, the $\sigma_{0.2}/M$ curves should be independent of α, i.e. horizontal lines. For the present material, it can be seen that texture has almost no effect on the anisotropy at low strains, and the observed flow stress anisotropy must be ascribed to other causes, i.e. to a microstructural anisotropy. At high strains, the situation is somewhat different. Here texture is the main, but not the only cause of the anisotropy. However, this is not always the case. An example of this is shown in Fig. 4. Here $\sigma_{0.2}/M$ curves are shown

for the same material as in Fig. 3, but the "Fig. 4 material" was, prior to rolling, heat treated to get a larger initial grain size. From Fig. 4 it is seen, that even at very large strains ($\varepsilon = 3.0$), texture effects cannot explain the anisotropy.

It has been argued that the Taylor model, used for the calculation of M, is too simple to describe the deformation conditions at large strains. To check whether this could be the explanation for the large strain results described above, M was also calculated using a more advanced model — the RC model — which should be more appropriate at the high strains [e.g. 10]. At high strains where the grain shape is non equiaxed, the Taylor criterion of the strain tensor being the same for all grains and being identical to the macroscopically applied one breaks down. In the RC-model the constraints of the grains is relaxed, i.e. every grains has a certain freedom to chose its shape change according to its orientation. A consequence of this is that the number of slip systems is reduced to 3 or 4 and that the number and combination of active slip systems may be different at grain interiors and at grain boundaries. It was found that the M-factors calculated using the RC model are lower than those of the Taylor calculation, however, the variation in M as a function of α is rather similar in the two cases. This can be seen from Fig. 4. Here $\sigma_{0.2}$/M-Taylor and $\sigma_{0.2}$/M-RC are shown. From the curves it can be concluded that independently of the model, Taylor or RC, a detailed analysis of anisotropy also at high strains must consider factors other than just texture.

Microstructure. Various elements in the microstructure can cause anisotropy, for example directionally of the grain shape and of second-phase particles as well as the presence of shear bands. Another cause is latent hardening, i.e. an increase in flow stress on the secondary slip systems because of interactions between dislocations on such systems and dislocations on the primary slip systems. For the present materials none of these effects give significant contributions to the observed anisotropies.

For high stacking fault fcc metals (e.g. aluminium) the deformation microstructure develops with strain from tangled dislocations to a regular cell structure with superimposed bands. For the present aluminium materials the observed bands are microbands - i.e. bands which separate volumes of materials deforming by different combinations of active slip systems [11]. Typically the microbands are 1-100 μm long and 0.1-1 μm wide. The crystallographic misorientation across a microband is typically 5-10° and the dislocation density within a band is much higher than in the surrounding cell structure. Examples are shown in Fig. 5. In general a microband is restricted to one original grain. In spite of this, the geometrical orientation of the microbands are almost identical from grain to grain; the variations are typically within a range of $\pm 10°$. At low strains (e.g. $\varepsilon = 0.2$) most of the microbands form on one system with orientations very similar to shear bands (see Fig. 6a), whereas at higher strains (e.g. $\varepsilon = 2.0$) the bands also form in a secondary direction (see Fig. 6b).

It is suggested that the microbands can interfere with the slip process and thus be a cause of anisotropy. At present, it is not possible to derive quantitative relations for the effects of microbands on either the absolute value of flow stress or the anisotropy. However, qualitatively there seem to be a good correlation between the observed microstructural anisotropy and the microbands. At low strains, where the microbands develop as a system of parallel walls, it is expected that the flow stress would increase as the angle between the rolling and the tensile direction is increased; which is in agreement with the experimental results. Tentatively the more complex microstructural anisotropy at large strains (Figs. 3 and 4) relates to the observation that the microbands form on two intersection planes. Further support for these interpretations is given in the next paragraph where the effects of metallurgical parameters on flow stress anisotropy and microstructural development are discussed.

Metallurgical parameters

The rolling strain has large effects on the flow stress anisotropy, the texture, the microstructure and

on the relative importance of texture/microstructure effects on the anisotropy. This has already been described above. Also other parameters are of importance. So far our investigations have been concentrated on these parameters: purity of the aluminium, initial grain size and deformation mode (normal and cross rolling). Clearly, other researchers have studied anisotropy in lots of other materials with other parameters, but as these latter studies do not cover all three aspects: flow stress anisotropy, texture and microstructure (in particular microband development), the present discussion is limited to our own results.

Table 1 and 2 give an overview of the microband development and the microstructural anisotropy, i.e. the flow stress anisotropy normalized for texture effects, for the various samples. When texture is not considered in the tables, it is because the effects of texture are relatively much more straightforward to calculate than those of microbands.

TABLE 1 - Overview of the effects of strain, purity, initial grain sizes and deformation mode on the microstructural anisotropy. " + " and " − " refer to anisotropy and no anisotropy, respectively. In the cases where anisotropy is observed, "I" refers to situations where $\sigma_{0.2}/M$ increases as a function of α over the entire 0-90° interval, whereas "P" refers to situations where $\sigma_{0.2}/M$ has a peak around $\alpha=40\pm10°$.

Strain	Purity		Grain Size		Deformation mode	
	99,996%	99.6%	fine	medium and coarse	normal rolling	cross rolling
low (e.g. $\varepsilon=0.2$)	+ (I)	+ (I)	+ (I)	+ (I)	+ (I)	−
high (e.g. $\varepsilon=2.0$)	−	+ (P)	−	+ (P)	+ (P)	−

TABLE 2 - Overview of the effects of strain, purity, initial grain size and deformation mode on the microband development. " + " and " − " refer to microbands and no microbands respectively. In the cases where microbands are observed, "1" refers to microbands on primarily one geometrical plane (Fig. 6a) and "2" refers to microbands on the two geometrical planes (Fig. 6a and b). * No or almost no microbands are observed in the rolling plane section.

Strain	Purity		Grain Size		Deformation mode	
	99,996%	99.6%	fine	medium and coarse	normal rolling	cross rolling
low (e.g. $\varepsilon=0.2$)	+ (1)	+ (1)	+ (1)	+ (1)	+ (1)	not macrosc. oriented
high (e.g. $\varepsilon=2.0$)	−*	+ (2)	−*	+ (2)	+ (2)	not macrosc. oriented

Purity. At low strains pure (99.996%) and commercially pure (99.6%-1100) aluminium behave rather similarly. Due to a fairly strong initial texture in the pure material the $\sigma_{0.2}$ versus α curves are somewhat different; the increase in flow stress with α is almost twice as big in the commercial purity material. However, when texture effects are taken into account, the two materials are almost identic; $\sigma_{0.2}/M$

increases about 16% when α is increased from 0° to 90°, and a regular microband structure develops in both materials (see tables 1 and 2).

At high strains the flow stress anisotropy in the two materials resemble each other but have different causes. In the commercial purity material, texture is, as already described, the main but not the only explanation for the anisotropy. Whereas, in the pure material, the total anisotropy relates to texture. A microstructural investigation of heavily deformed pure aluminium in the rolling plane section revealed no microbands [7]. An inspection of the longitudinal plane section (containing RD and ND), however, showed that the typical microband structure — as described above — at the high strain is almost completely replaced by another structure consisting of elongated subgrains delineated by extended subgrain walls which are almost parallel to the rolling direction. From these results, it is concluded that i) the primary set of macroscopically oriented microbands (Fig. 6a) disappear in pure aluminium deformed to high strains, probably due to recovery effects being enhanced by the increase in purity and ii) that the walls parallel to the rolling plane seem to have no major influence on the flow stress anisotropy (as measured in the rolling plane).

Grain size. Compared to a medium grain size (80 µm) 99.6% material a finer grain size (35 µm) material has the similar type but less anisotropy at low strain. And, as the fine grained material had a stronger initial rolling type texture, the *microstructural* anisotropy is even more weak in the fine grained material. This again correlates well with the microband development. The tendency to form parallel microbands is less pronounced in the fine grained material, the microbands do form, but they are curled and bend due to grain-grain interactions in the grain boundary zones.

At high strains, the flow stress anisotropy in the fine grained material is stronger but of the same type as that in the coarse grained material. But, as for the pure material, this strong anisotropy can be ascribed to texture. Practically no microbands are observed in the rolling plane section of the heavily deformed fine grained material. An inspection of the longitudinal plane section has not been done. However, also based on the results for pure aluminium, the lack of microstructural anisotropy seem to correlate well with the observation that no microbands oriented as sketched in Fig. 6a are present.

Deformation mode. Two deformation modes — normal cold rolling and cold cross rolling — was used. It has to be emphasized that the cross rolling was introduced in the present series of experiments not to simulate industrial processing (our scales are much smaller) but to introduce a different microstructural evolution. At low strains the flow stress anisotropy in the cross rolled material is much weaker than in the normal rolled material, only about 6% as compared to 20%, and texture can explain the "cross rolled anisotropy". Microbands do develop in the rolled material. However, they are not well organized along one or two macroscopic directions as in the normal rolled material, but are curled and bend in very many directions with respect to the sample axis. An example is shown in Fig. 7. I.e., as the microbands are so disorganized they are not expected to have significant influences on the micostructural flow stress anisotropy.

At high strains the cross rolled material is almost isotropic (variation less than 3%) and when texture effects are taken into account the variations are less than the experimental uncertainty. Only preliminary microstructural investigations of the rolling plane section have so far been carried out, however, they show that microbands exist but are oriented over a wide range of angles with respect to the sample axis.

Conclusions

The present analysis of flow stress anisotropy in cold-rolled aluminium shows a significant effect of both the crystallographic texture and the microstructure. It also shows the effect of process and materials parameters on texture, microstructure and properties in the cold-deformed state. These findings have

some general implications for the materials behaviour during forming operations. Of special importance is the microstructural observations showing that the microstructural evolution is heterogeneous, i.e. the plastic strain is not uniform; however many structural features (e.g. dense dislocation walls and microbands) are observed to be organized on a macroscopic scale. This structure evolution may relate both to surface changes observed during forming as well as to the occurrence of localized shear. The microstructural evolution is markedly influenced by process and materials parameters and an analysis of such effects will be useful in interpreting observations of the effect of similar parameters on forming operations.

References

[1] Lequeu, P. and Jonas, J.J. Modelling of the plastic anisotropy in textured sheet. *Met. Trans. A*, 19A (1988), 105-120.

[2] Kocks, U.F. Stout, M.G. and Rollett, A.D. The influence on texture on strain hardening. P.O. Kettunen et al. (Eds.), *Strength of Metals and Alloys*, Pergamon, Oxford, 1988, Vol. 1, pp. 25-34.

[3] Rollett, A.D., Canova, G.R. and Kocks, U.F. The effect of the cube texture component on the earing behaviour of rolled fcc metal. A.K. Sachdev and J.D. Embury (Eds.), *Formability and Metallurgical Structure*, TMS, NY, 1987, pp. 147-157.

[4] Kallend, J.S. and Davies, G.J. The elastic and plastic anisotropy of cold-rolled sheets of copper, gilding metal and α-brass. *J. Inst. Metals*, 5 (1971), 257-260.

[5] Martin, P., Baudelet, B., Espérance, G.L., Korbel, A. and Schmitt, J.H. Macroscopic strain localization: role of microstructural instabilities. P.O. Kettunen et al. (Eds.), *Strength of Metals and Alloys*, Pergamon, Oxford, 1988, Vol. 1, pp. 403-408.

[6] Raphanel, J.L., Schmitt, J.H. and Baudelet, B. Plastic behaviour of prestrained materials: experiments and analysis through a simple model. S.I. Andersen et al. (Eds.), *Constitutive Equations and their Physical Basis*, Risø, Roskilde, 1987, pp. 491-496.

[7] Juul Jensen, D. and Hansen, N. Flow stress anisotropy in aluminium. *Acta metall. et mat.*, 38 (1990), 1369-1380.

[8] Juul Jensen, D. and Hansen N. Relations between texture and flow stress in commercially pure aluminium. S.I. Andersen et al. (Eds.), *Constitutive Equations and their Physical Basis*, Risø, Roskilde, 1987, pp. 353-360.

[9] Taylor, G.I. Plastic Strain in Metals. *J. Inst. Metals*, 62 (1938), 307-324.

[10] Mecking, H. Deformation of polycrystals. P. Haansen et al. (Eds.), *Strength of Metals and Alloys*, Pergamon, Toronto, 1980, Vol. 3, 1573-1594.

[11] Bay, B., Hansen, N. and Kuhlmann-Wilsdorf, D. Deformation structures in lightly rolled pure aluminium. *Mat. Sci. Eng.*, A113 (1989), 385-397.
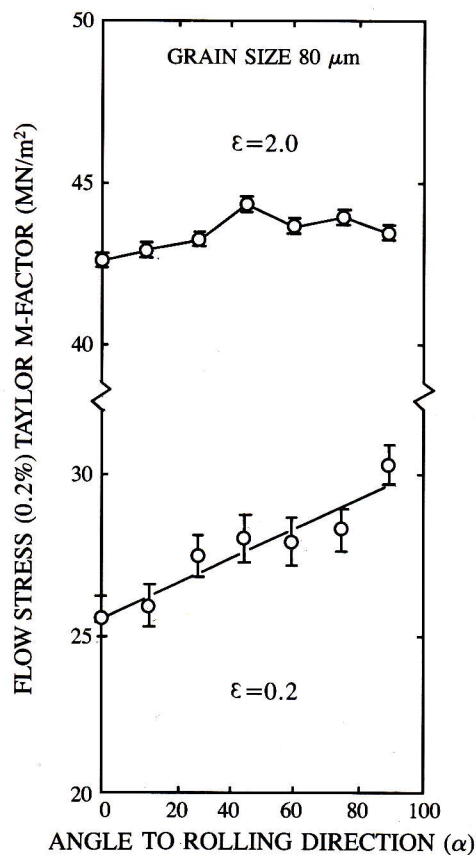
Fig. 1:
Angular variation of the flow stress (0.2% offset) in the rolling plane for commercially pure aluminium with an initial grain size of 80 μm deformed to ε = 0.2 and ε = 2.0 by cold rolling. (The error bars are calculated as average values for all measurements at a given strain).
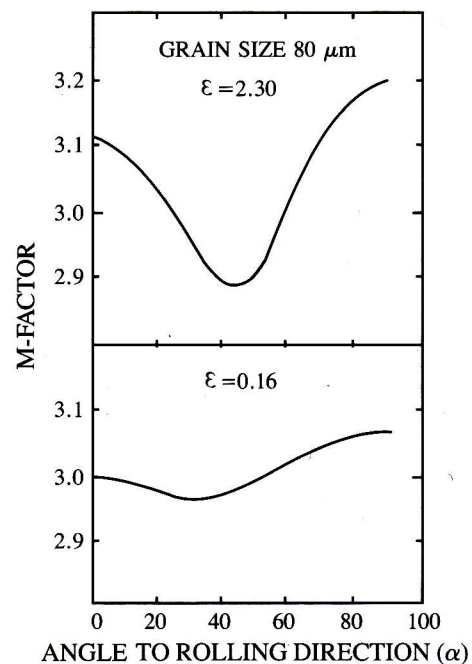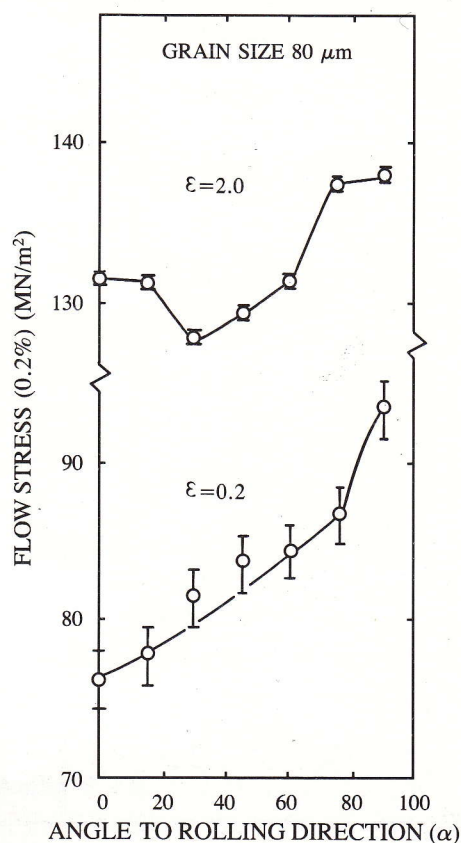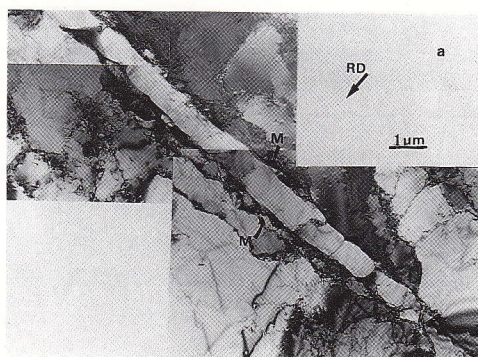

Fig. 2:
Angular variation of the Taylor M-factor in the rolling plane for commercially pure aluminium with an initial grain size of 80 μm deformed to ε = 0.16 and ε = 2.30 by cold rolling.
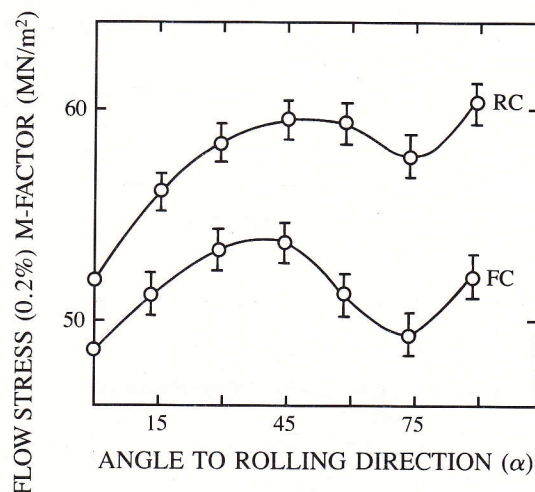
Fig. 3:
Angular variation of the flow stress divided by the corresponding Taylor M-factor for commercially pure aluminium with an initial grain size of 80 μm deformed to ε = 0.2 and ε = 2.0 by cold rolling. (The error bars are calculated as average values for all measurements at a given strain).

Fig. 4:
Angular variation of the flow stress divided by the corresponding M-factor for commercially pure aluminium with an initial grain size of 400 μm deformed ε = 3.0 by cold rolling. The two curves refer to two M-factor calculation theories: FC to the Taylor model, RC to the relaxed constraint model.
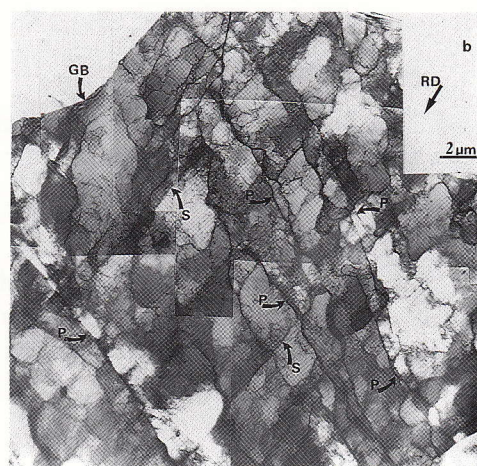

Fig. 5a:
Microstructure as seen in a TEM foil parallel to the rolling plane of commercially pure Al deformed to ε = 0.2 by cold rolling. Parallel microbands are marked by M. The rolling direction is labelled RD.

Fig. 5b:
Thin foil parallel to the longitudinal plane of pure Al deformed to ε = 0.2. Microbands (and dense dislocation walls) are seen on two intersecting planes (marked P and S). An original grain boundary is identified as GB and the rolling direction is along RD.
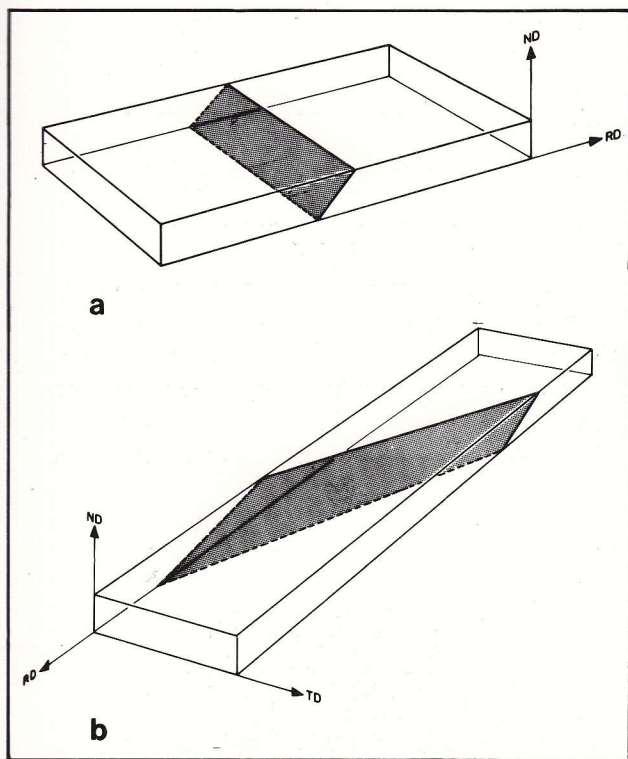
Fig. 6:
Schematic drawing of the geometrical orientation of the microbands with respect to the sample axes. a) Primary microband plane. b) Secondary microband plane.
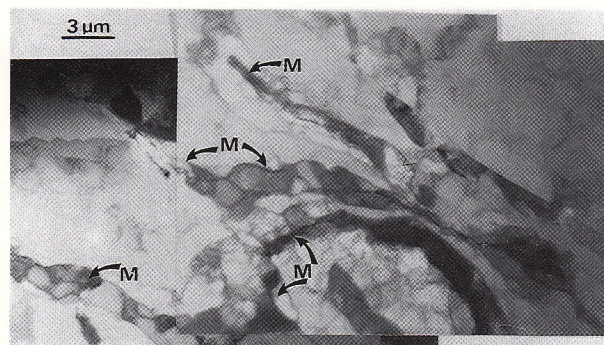

Fig. 7:
Microstructure as seen in a TEM foil parallel to the longitudinal plane of commercially pure Al deformed to $\varepsilon = 0.2$ by cross rolling. Microbands are marked by M.